Electromagnetic properties of the rotationally aligned band in ^{162}Dy

C. Y. Wu, D. Cline, M. W. Simon, G. A. Davis, and R. Teng
Nuclear Structure Research Laboratory, Department of Physics, University of Rochester, Rochester, New York 14627

A. O. Macchiavelli and K. Vetter
Nuclear Science Division, Lawrence Berkeley National Laboratory, Berkeley, California 94720

(Received 27 July 2001; published 20 November 2001)

Rotational band structures in ^{162,164}Dy were studied by projectile inelastic excitation on a ^{118}Sn target at near-barrier energies. States with spin up to $24^+(22^+)$ of the ground-state band and $18^+(18^+)$ of the γ-vibrational band in ^{162}Dy(^{164}Dy) were populated in these reactions. States with spin spanning from 8^+ to 20^+ of the rotationally aligned S band in ^{162}Dy were populated by way of its band-crossing point with the γ-vibrational band at spin 12^+, where strong mixing occurred due to an accidental degeneracy. This S band eventually crosses the ground-state band at spin 18^+ and becomes the yrast at spin 20^+. From the peripheral-collision γ-ray yield data, sets of electromagnetic matrix elements for both the intraband and interband transitions were determined by using the Coulomb excitation code, GOSIA. The measured intraband $E2$ matrix elements were used to derive a quadrupole deformation of the S band that is $\approx$20% larger than those of the nearby low-lying collective bands. This represents the first measurement made for the quadrupole deformation of the S band for states well below the crossing point with the ground-state band. The two-phonon γ-vibration harmonic strength in ^{162}Dy is highly fragmented, 36% of the strength is located in two $K^\pi=4^+$ bands at excitation energies 1535.9 and 2181.0 keV, respectively. Significant octupole collectivity was observed coupling the ground-state band to the $K^\pi=2^-$ band in ^{162}Dy.

DOI: 10.1103/PhysRevC.64.064317 PACS number(s): 21.10.Ky, 21.10.Re, 27.70.+q

I. INTRODUCTION

A sharp change in the moment of inertia for the rotational band along the yrast sequence in deformed nuclei is believed to be caused by the intersection of a rotationally aligned S band and the ground-state band [1]. The degree of sharpness in the change of the moment of inertia depends on the interaction strength between these two bands, which is a function of the degree of filling of the high-j orbit occupied by the aligned two quasiparticles in the S band [2,3]. This rotationally induced alignment of the angular momentum of a pair of decoupled particles is an important manifestation of the Coriolis interaction in nuclei. Many related issues on other aspects of the interplay between the single-particle and the collective motions also can be addressed by study of the S band. For example, the gradual reduction of collectivity of the S band beyond the crossing point, derived from the measured lifetimes, strongly suggests that a shape evolution, from prolate through triaxial to oblate, occurs [4–6] because of the gradual dominance of the single-particle motion in the contribution to the total angular momentum.

Most of the spectroscopic data available for these aligned two-quasiparticle bands are for states near or above the crossing point in mainly neutron-deficient nuclei. This is because the heavy-ion fusion-evaporation reaction, which is the main experimental method used to study this phenomenon, favors the formation of the neutron-deficient nuclei and the decay mechanism favors the path along the yrast sequence. The only exception is for the low-spin members of the S band in the stable nucleus, ^{160}Dy, where candidates for the 4^+, 6^+, and 8^+ members were identified by the $(\alpha,^3\mathrm{He})$ reaction [7]. The electromagnetic properties for the S band members below the crossing point were basically unknown prior to the present work although limited electromagnetic properties for the S band in ^{164}Er were obtained in an early Coulomb excitation [8].

In this paper, we present a unique case where members of the S band, with spin ranging from 8^+ to 20^+, were populated by Coulomb excitation. This provides, for the first time, extensive data on the electromagnetic properties and also the locations of the S band members below the crossing with the ground-state band. In addition, other aspects of collectivity, such as the two-phonon γ-vibrational strength and both the dipole and octupole strengths to the negative-parity states, were measured in the same experiment.

Following submission of this paper, preliminary results of a study of high spin states populated via the incomplete fusion reaction was reported in conference proceedings by Jungclaus *et al.* [9]. The incomplete fusion reaction work populated high spin states to similar or higher spin to those seen in the present work, and the agreement between these separate studies is excellent. However, the Coulomb excitation population mechanism differs significantly from that for incomplete fusion, leading to different focus for the physics implications. The incomplete fusion study focused on the band interaction strengths, whereas the present Coulomb excitation study emphasizes the electromagnetic properties of the interacting bands.

II. EXPERIMENTS

A highly enriched ^{118}Sn target, with 99.975% isotope abundance, was bombarded by a ^{162}Dy beam at $E_{lab}=780$ MeV (790 MeV for ^{164}Dy), provided by the 88 in. Cyclotron facility at the Lawrence Berkeley National Laboratory. The projectile and target combination was chosen to

optimize the study of multinucleon transfer reactions between a spherical and a deformed nucleus. Results on the two-neutron transfer reaction leading to the production of the neutron-rich nuclei have been published in a previous paper [10].

The target with thickness $\approx 250\ \mu g/cm^2$ was prepared by evaporating ^{118}Sn onto a carbon foil of $\approx 20\ \mu g/cm^2$ and overcoating with aluminum of $\approx 6\ \mu g/cm^2$ thick. Scattering angles of both the projectilelike and targetlike nuclei, plus their time-of-flight difference, were measured by the highly segmented parallel-plate avalanche detector array, CHICO [11], which covers scattering angles θ from 20° to 85° and 95° to 168° relative to the beam axis and an azimuthal angle ϕ totaling 280° out of 360°. Valid events required the coincident detection of both scattered nuclei and at least one γ-ray detected by GAMMASPHERE using 100 Ge detectors. A total of 7.0×10^8 events were collected for ^{162}Dy in about 66 h with an average beam intensity of about 1 particle nA; about 4% of these events have a γ-ray fold of three or more. A total of 0.23×10^8 events were collected for ^{164}Dy in about 4 h with an average beam intensity of 0.6 particle nA.

Reconstruction of events from the measured two-body kinematics allows the determination of masses of the reaction products, velocity vectors, and Q value. CHICO achieved an angle resolution of about 1° in θ and 9.3° in ϕ, and a time resolution of about 500 ps, leading to a mass resolution, $\Delta m/m$, of about 5%, which is similar to the resolution reported previously [12–14]. This mass resolution is sufficient to distinguish projectilelike from targetlike nuclei and appropriate Doppler-shift corrections for the detected γ rays can be applied. The typical resolution for the total Doppler-corrected γ-ray spectrum is about 1.0%. Shown in Fig. 1 are the raw γ-ray spectrum and Doppler-shift corrected spectrum for both the targetlike and projectilelike nuclei for the angular range of $60°<\theta_{\mathrm{c.m.}}<100°$.

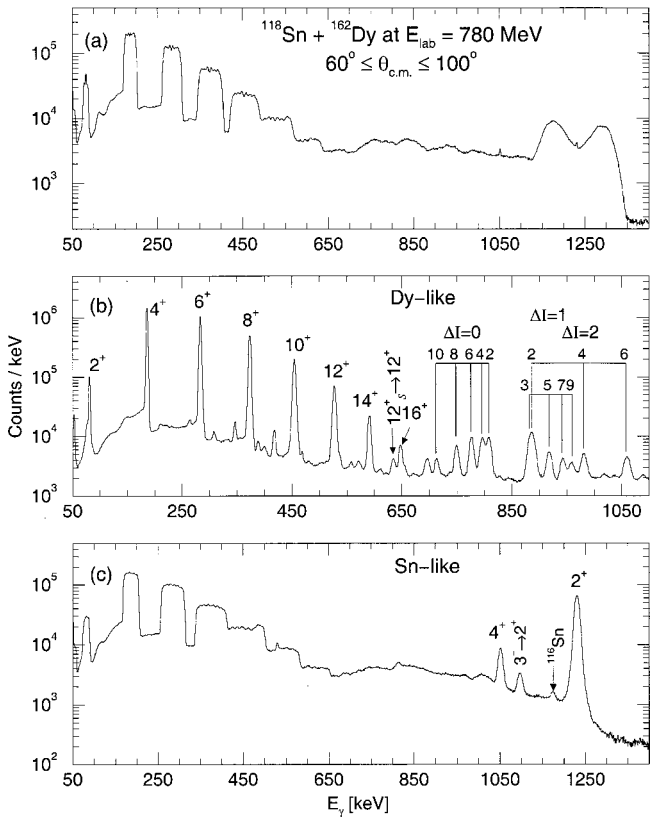

FIG. 1. The raw γ-ray spectrum for the reaction between a ^{118}Sn target and a ^{162}Dy beam is shown in (a) together with Doppler-shift corrected ones for the projectilelike particle (b) and the targetlike particle (c). The labeled peaks are the $I\rightarrow(I-2)$ transitions for the inelastic channel unless specified. The interband transitions between the γ and ground-state bands are grouped by $\Delta I=0$, 1, 2 as indicated in (b).

III. RESULTS

The level structure of ^{162}Dy has been studied extensively and has been categorized into 16 rotational bands [15], which include the ground-state, γ-vibrational, $K^\pi=4^+$, and $K^\pi=0^-$, 1^-, 2^-, and 3^- octupole-vibrational bands among others. The ground-state band was extended from spin 18^+ [16] up to 24^+ at 6153.5 keV, while states with spin up to 18^+ of the $K^\pi=2^+$, γ-vibrational band and 12^- of the $K^\pi=2^-$, octupole-vibrational band were populated. The known $K^\pi=4^+$ band at 1535.9 keV was extended from spin 7^+ to spin 16^+ at 3835 keV, while a new $K^\pi=4^+$ band at 2181.0 keV was identified up to spin 6^+ by this work and the work of Bauer [17]. States with spin ranging from 8^+ to 20^+ of the S band were populated in this work and with spin up to 28^+ were identified by the work of Jungclaus *et al.* [9] and Bauer [17]. Current work is the first case where an extended sequence of the S band, below the crossing with the ground-state band, has been populated by Coulomb excitation and their electromagnetic properties have been determined. All the transitions and level placements were identified by events having at least three γ rays.

The level scheme of the ground-state, γ-vibrational, and S bands and the observed transitions from this experiment are shown in Fig. 2, where the complex band intersections of the S band with the ground-state band at spin 18^+ and with the γ-vibrational band at spin 12^+ can be seen. The interband transitions between the γ-vibrational and the ground-state band are not shown in the figure for clarity, but their relative intensities are listed in Table I. The agreement with the Ref. [15] is reasonable except for the 10^+_γ decay. The relative γ-ray intensities for the decay of the S band members are listed in Table II. The level scheme of the $K^\pi=2^-$ octupole-vibrational and two $K^\pi=4^+$ bands, and their couplings to the γ-vibrational band are shown in Fig. 3. The relative γ-ray decay intensities for members of two $K^\pi=4^+$ bands are listed in Table III. Note that the level scheme of both the γ-vibrational and the S bands has been modified and extended significantly for states with spin 12^+ and above from the previous work [18]. Also the $\Delta I=2$ transitions to the ground-state band for the 8^+ state at 1985.9 keV and 10^+ state at 2262.3 keV of the S band, seen in the early work [18], were not observed in this experiment.

For ^{164}Dy, the known level scheme for both the ground-state and γ-vibrational bands [19] was extended significantly by the current work. The ground-state band was extended from spin 14^+ to spin 22^+ at 4932.0 keV while the

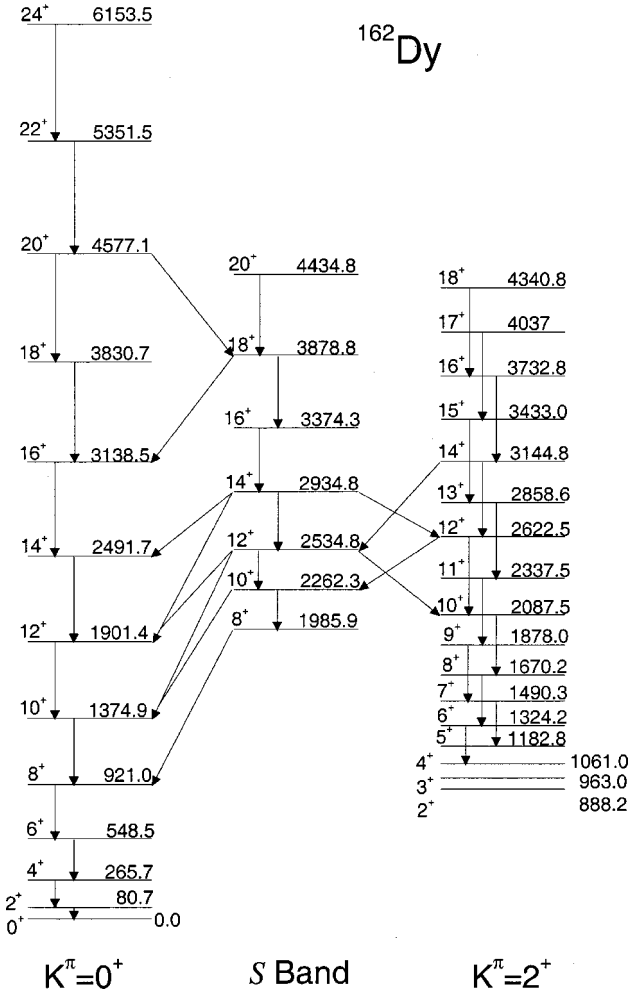

FIG. 2. Level scheme for the ground-state, γ-vibrational, and S bands of ^{162}Dy derived from the current work. For clarity, the interband transitions between the γ-vibrational and the ground-state band are not shown but their relative γ-ray decay branchings are listed in Table I.

γ-vibrational band was extended from spin 6^+ to spin 18^+ at 4037.8 keV. The level scheme and the observed transitions from current experiment are shown in Fig. 4. The relative intensities for the γ-ray decay of the γ-vibrational band members are listed in Table IV.

IV. ANALYSIS AND DISCUSSION

Prior knowledge of the absolute $E\lambda$ strengths for ^{162,164}Dy was limited to the band heads of collective bands, except for the ground-state band where the $B(E2)$ values or the lifetimes for states with spin up to 18^+ in ^{162}Dy [16] and 14^+ in ^{164}Dy [20] were measured by the Coulomb excitation experiments. The current work, which benefits from significantly improved detection efficiency for both particles and γ rays, expands our knowledge of the electromagnetic properties not only to states with higher spin, but also to more exotic structures, such as the quadrupole deformation of the low-spin members of the rotationally aligned S band.

It has long been recognized that Coulomb excitation is an ideal experimental method to study collective aspects of nuclei but it is not useful for studying the S band because there are no connecting paths having collective strength to the low-lying states. Therefore, the finding of the population of

TABLE I. Relative γ-ray intensity for the decay of the γ band in ^{162}Dy.

Transition	E_γ (keV)	Relative intensity	
		This work	Ref. [15]
$2_\gamma \rightarrow 0_1$	888.2	0.87(6)	0.90(4)
$2_\gamma \rightarrow 2_1$	807.5	1.00	
$3_\gamma \rightarrow 2_1$	882.3	6.83(49)	5.21(22)
$3_\gamma \rightarrow 4_1$	697.3	1.00	
$4_\gamma \rightarrow 2_1$	980.3	0.62(4)	0.57(5)
$4_\gamma \rightarrow 4_1$	795.3	1.00	
$5_\gamma \rightarrow 4_1$	917.1	6.60(48)	5.32(68)
$5_\gamma \rightarrow 6_1$	634.3	1.00	
$6_\gamma \rightarrow 4_1$	1058.5	0.60(4)	0.73(9)
$6_\gamma \rightarrow 6_1$	775.7	1.00	
$6_\gamma \rightarrow 4_\gamma$	263.2	0.137(13)	0.13
$7_\gamma \rightarrow 6_1$	941.8	5.39(42)	
$7_\gamma \rightarrow 8_1$	569.3	1.00	
$7_\gamma \rightarrow 5_\gamma$	307.5	1.62(16)	
$8_\gamma \rightarrow 6_1$	1121.7	0.91(13)	0.53
$8_\gamma \rightarrow 8_1$	749.2	1.00	
$8_\gamma \rightarrow 6_\gamma$	346.0	0.62(4)	0.50
$9_\gamma \rightarrow 8_1$	957.0	1.00	
$9_\gamma \rightarrow 7_\gamma$	387.7	0.49(5)	
$10_\gamma \rightarrow 8_1$	1166.5	0.97(12)	
$10_\gamma \rightarrow 10_1$	712.6	1.00	
$10_\gamma \rightarrow 8_\gamma$	417.3	1.81(13)	9.5
$12_\gamma \rightarrow 10_1$	1247.6	3.37(51)	
$12_\gamma \rightarrow 12_1$	721.1	1.00	
$12_\gamma \rightarrow 10_\gamma$	535.0	6.64(93)	
$12_\gamma \rightarrow 10_s$	360.2	0.84(42)	
$14_\gamma \rightarrow 12_1$	1243.4	0.26(11)	
$14_\gamma \rightarrow 12_\gamma$	522.3	1.00	
$14_\gamma \rightarrow 12_s$	610.0	< 0.86	

TABLE II. Relative γ-ray intensity for the decay of the S band in ^{162}Dy.

Transition	E_γ (keV)	Relative intensity
		This work
$10_s \rightarrow 10_1$	887.4	2.7(13)
$10_s \rightarrow 8_s$	276.4	1.00
$12_s \rightarrow 10_1$	1159.9	1.36(16)
$12_s \rightarrow 12_1$	633.4	1.00
$12_s \rightarrow 10_\gamma$	447.3	1.96(22)
$12_s \rightarrow 10_s$	272.3	0.122(17)
$14_s \rightarrow 12_1$	1033.4	0.21(6)
$14_s \rightarrow 12_s$	400.0	1.00
$14_s \rightarrow 14_1$	443.1	0.22(3)
$14_s \rightarrow 12_\gamma$	312.3	0.051(8)

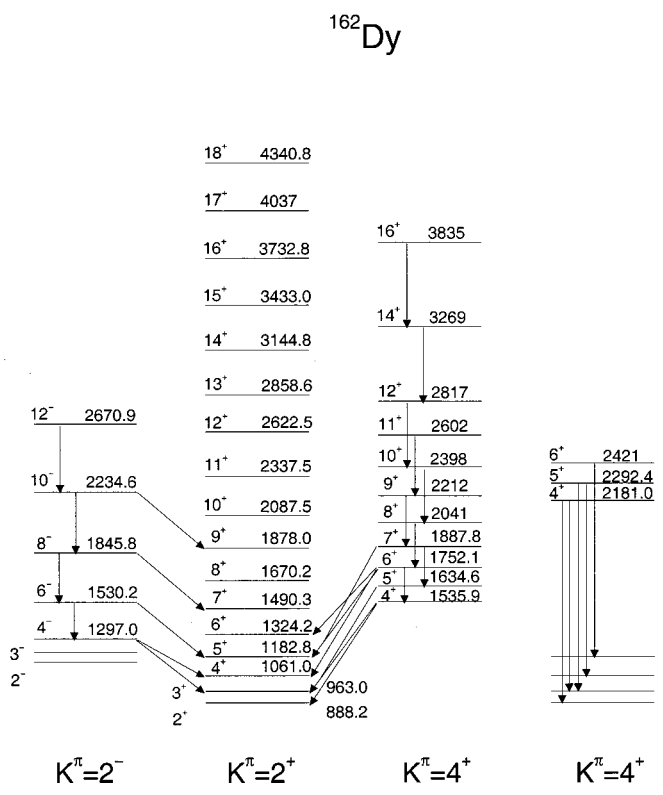

FIG. 3. Level scheme for the $K^{\pi}=2^{-}$ octupole-vibrational band and the known, plus a new, $K^{\pi}=4^{+}$ band of ^{162}Dy. Note that the spin 12^{-} state of the $K^{\pi}=2^{-}$ band has a different energy from that quoted in a previous work [18].

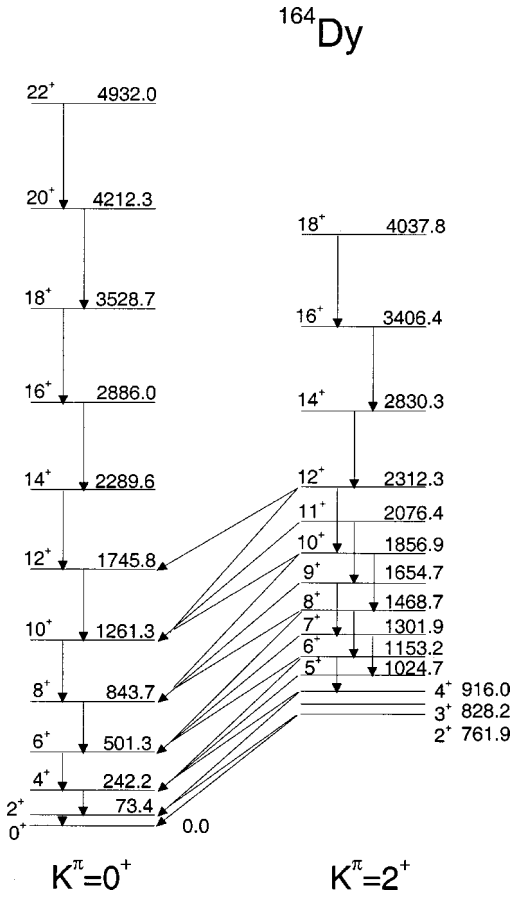

FIG. 4. Level scheme for the ground-state and γ-vibrational bands of ^{164}Dy together with the observed transitions from the current experiment.

the *S* band via Coulomb excitation of ^{162}Dy came as a surprise. In particular, population of the low-spin region cannot be reached easily by other experimental methods. A strong mixing between the *S* and γ-vibrational bands at spin 12^{+} opens a viable avenue for Coulomb excitation of the *S* band and a rare opportunity to study its collective properties well below the crossing with the ground-state band. The discontinuity at spin 12^{+} in the dependence of moment of inertia on rotational frequency for both the γ-vibrational and *S* bands, shown in Fig. 5, is evidence for the strong mixing at the band crossing. The nearly constant moment of inertia for the *S* band is about twice that of the ground-state band. This *S* band crosses the ground-state band at spin 18^{+} and becomes yrast at spin 20^{+} (see Fig. 2).

TABLE III. Relative γ-ray intensity for the decay of the two $K^{\pi}=4^{+}$ bands in ^{162}Dy. Subscript 4 is for the band at excitation energy 1535.9 keV and subscript 5 at excitation energy 2181.0 keV.

Transition	E_{γ} (keV)	Relative intensity	
		This work	Ref. [15]
$4_4 \rightarrow 2_{\gamma}$	647.7	1.00	
$4_4 \rightarrow 3_{\gamma}$	572.9	0.68(15)	0.55(5)
$5_4 \rightarrow 3_{\gamma}$	647.7	1.00	
$5_4 \rightarrow 4_{\gamma}$	572.9	0.81(46)	2.50(22)
$6_4 \rightarrow 4_{\gamma}$	691.1	2.01(63)	
$6_4 \rightarrow 5_{\gamma}$	569.3	3.2(10)	0.53(8)
$6_4 \rightarrow 6_{\gamma}$	427.9	1.00	
$4_5 \rightarrow 2_{\gamma}$	1292.8	1.00	
$4_5 \rightarrow 3_{\gamma}$	1218.0	1.13(24)	
$5_5 \rightarrow 3_{\gamma}$	1329.4	1.00	
$5_5 \rightarrow 4_{\gamma}$	1231.4	2.15(70)	

The analysis to extract the electromagnetic matrix elements from the experimental γ-ray yields was done using the Coulomb excitation code, GOSIA [21,22], which allows one to search for the best set of electromagnetic matrix elements by fitting the calculated to the experimental γ-ray yields. Precautions were taken in the analysis to ensure that the scattering angular range used in the Coulomb excitation analysis is not appreciably perturbed by Coulomb-nuclear interference effects. A comparison between the experimental yields and Coulomb excitation predictions over a wide range of scattering angles was used to identify the onset of Coulomb-nuclear interference effects. Figure 6 shows a comparison of γ-ray yields between prediction and experiment for the intraband transitions of both the ground-state and γ-vibrational bands in ^{164}Dy over three partitions of scattering angle. Only two sets of data were included in the determination of electromagnetic matrix elements; that is, the scattering angle ranges $22.2°-29.2°$ and $30.0°-35.0°$, because a consistent fit could not be obtained for the data with an angular range

TABLE IV. Relative γ-ray intensity for the decay of the γ band in ^{164}Dy.

Transition	E_γ (keV)	Relative intensity	
		This work	Ref. [19]
$2_\gamma \rightarrow 0_1$	761.4	1.00(7)	0.87(3)
$2_\gamma \rightarrow 2_1$	688.3	1.00	
$3_\gamma \rightarrow 2_1$	754.4	5.67(44)	5.55(93)
$3_\gamma \rightarrow 4_1$	585.3	1.00	
$4_\gamma \rightarrow 2_1$	842.2	0.68(5)	0.62(6)
$4_\gamma \rightarrow 4_1$	673.6	1.00	
$5_\gamma \rightarrow 4_1$	782.0	6.83(61)	9.1(17)
$5_\gamma \rightarrow 6_1$	523.1	1.00	
$6_\gamma \rightarrow 4_1$	910.9	0.69(5)	
$6_\gamma \rightarrow 6_1$	652.0	1.00	
$6_\gamma \rightarrow 4_\gamma$	237.5	0.15(1)	
$7_\gamma \rightarrow 6_1$	800.4	1.00	
$7_\gamma \rightarrow 5_\gamma$	277.8	0.36(3)	
$8_\gamma \rightarrow 6_1$	967.7	0.92(7)	
$8_\gamma \rightarrow 8_1$	625.5	1.00	
$8_\gamma \rightarrow 6_\gamma$	315.5	0.93(9)	
$9_\gamma \rightarrow 8_1$	810.9	1.00	
$9_\gamma \rightarrow 7_\gamma$	352.4	0.84(18)	
$10_\gamma \rightarrow 8_1$	1013.9	0.80(10)	
$10_\gamma \rightarrow 10_1$	596.1	1.00	
$10_\gamma \rightarrow 8_\gamma$	388.2	3.46(42)	
$12_\gamma \rightarrow 10_1$	1052.5	0.74(12)	
$12_\gamma \rightarrow 12_1$	567.3	1.00	
$12_\gamma \rightarrow 10_\gamma$	455.3	< 22	

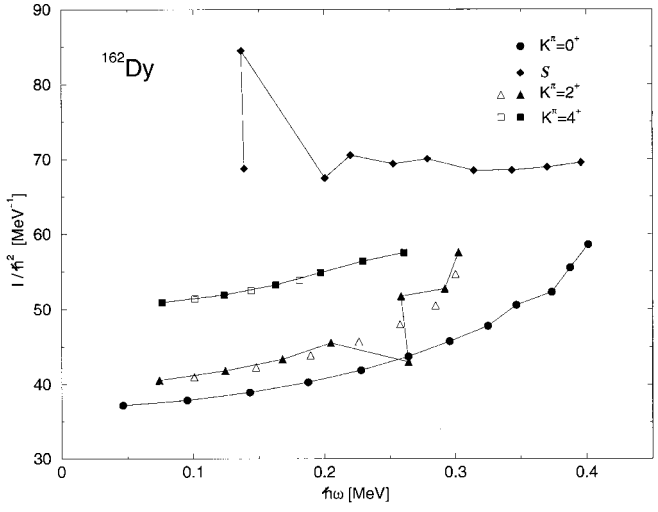

FIG. 5. The kinematical moment of inertia as a function of the rotational frequency for the ground-state, γ, $K^\pi=4^+$, and S bands. The convention used in calculating the moment of inertia and rotation frequency is from Ref. [27]. The level repulsion between the S and γ bands at spin 12^+ is indicated by the sudden shift of the moment of inertia in the plot. The data above spin 20^+ for the S band come from Refs. [9,17].

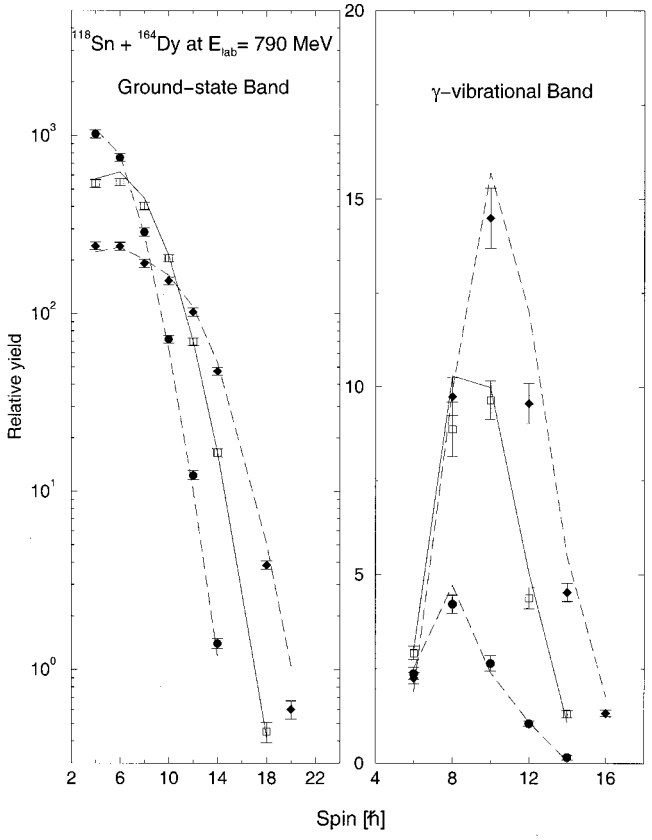

FIG. 6. Comparison of the γ-ray yields between the prediction and experiment for the $\Delta I=2$ intraband transitions of both the ground-state and the γ-vibrational bands in ^{164}Dy. The solid circles are the data for the angular range between 22.2° and 29.2°, the open squares for the angular range between 30.0° and 35.0°, and the solid diamonds for the angular range between 35.7° and 42.4°. The solid and dashed lines are the Coulomb excitation calculations for the best fits to the data.

between 35.7° and 42.4°, where the onset of Coulomb-nuclear interference effect occurs.

The available independent data from the current experiment is less than the number of unknown electromagnetic matrix elements to be determined, thus a strategy had to be used to limit the number of free parameters in the fits to avoid a runaway minimization. Matrix elements were coupled together wherever is possible, using observed systematics, to reduce the number of free parameters. For example, the $M1$ components for the $\Delta I=0$ or 1 transitions between the γ-vibrational and ground-state bands are generally small and the $E2$ components are correlated well with those of $\Delta I=2$ transitions by the equation [Eq. (4-210) in Ref. [23]]

$$\sqrt{B(E2,I_{K'}\rightarrow I_K)}=\langle I_{K'}K'2-2|I_KK\rangle[M_1-M_2\{I_K(I_K+1)-I_{K'}(I_{K'}+1)\}]\xi, \quad (1)$$

where M_1 and M_2 are the fitting parameters, $K'=K+2$ and $\xi=\sqrt{2}$ if $K=0$ and $\xi=1$ otherwise. Thus, the $M1$ matrix elements can be ignored and the whole set of the interband $E2$ matrix elements can be reduced to one free parameter,

TABLE V. Intrinsic matrix elements for the intraband transitions of both the ground-state and γ bands and for the interband transitions between those two bands in ^{162,164}Dy.

Nucleus	$\langle K=0\|E2\|K=0\rangle$ (e b)	$\langle K=2\|E2\|K=2\rangle$ (e b)	$\langle K=2\|E2\|K=0\rangle$ (e b)	M_2/M_1
^{162}Dy	2.18	2.19	0.245	−0.0121
^{164}Dy	2.23	2.24	0.250	−0.0128

that is the absolute strength, with the ratio of M_2/M_1 fixed by the observed branching ratios. Note that the intrinsic matrix elements between bands are related to M_1 and M_2 by the equation [Eq. (4-211) in Ref. [23]]

$$\langle K'|E2|K\rangle = M_1 + 4(K+1)M_2. \tag{2}$$

It is reasonable to assume that the $E2$ matrix elements within a band are correlated by the rotational relationship and driven by one free parameter, that is, the intrinsic matrix element. Two such parameters, one each for the ground-state and γ-vibrational bands, and one additional parameter for the interband intrinsic matrix element between the ground-state and γ-vibrational bands, were used in the fit of the γ-ray yields in ^{164}Dy. These determined $E2$ intrinsic matrix elements for ^{162,164}Dy are listed in Table V. They have an uncertainty that is less than 5%. The best fit of the γ-ray yields between the calculation and experiment is shown in Fig. 6 where the normalized $\chi^2=1.52$. A good agreement is reached for the spin up to 18^+ of the ground-state band and up to 14^+ of the γ-vibrational band.

The strong mixing of the S band in ^{162}Dy with the γ-vibrational band complicated the analysis compared to the case for ^{164}Dy. In ^{162}Dy both the intraband and interband transitions for states with spin 12^+ and 14^+ of the γ-vibrational band were treated as free parameters, rather than using the coupling scheme, but the relative strengths for a given state still were fixed according to the observed branching ratios. The same principle was applied to the transitions for the S band members. For the $\Delta I=0$ transitions between the S and ground-state bands, the dominant component was measured to be $M1$ for both the 8^+ and 10^+ states by Fields *et al.* [18], and was confirmed by our angular distribution data. The dominant $M1$ component also was suggested by our data for the $\Delta I=0$ interband transitions from the 12^+ and 14^+ states. The measured branching ratios of the $\Delta I=0$ interband transition relative to the $\Delta I=2$ intraband transition showed that these $M1$ matrix elements are correlated well by the equation [Eq. (4-254) in Ref. [23]]

$$\langle I_{K'}, K'=0_s\|M1\|I_K, K=0_1\rangle = (3/4\pi)^{1/2}(e\hbar/2Mc) \times \langle 0_s|g_R|0_1\rangle [(2I_K+1)I_1(I_K+1)]^{1/2}\delta(I_K, I_{K'}), \tag{3}$$

where g_R is an operator in the intrinsic frame and assuming $K=0$ for the S band. The index s is for the S band and the index 1 for the ground-state band. The determined matrix element for $\langle 0_s|g_R|0_1\rangle = 0.024(7)$. This corresponds to a $B(M1; 8_s^+ \rightarrow 8_1^+) = 0.0058$ W.u. A sample fit of the experimental γ-ray yields to predictions for both the ground-state and S bands is shown in Fig. 7, and for the γ-vibrational band is shown in Fig. 8 the normalized $\chi^2=1.54$. Good agreement is achieved for spins up to 20^+ of the ground-state band and up to 16^+ of both the S and γ-vibrational bands.

The measured intrinsic $E2$ matrix elements for both the ground-state and γ-vibrational bands are listed in Table V. The individual $E2$ matrix elements for the intraband transitions of the S band are shown in Fig. 9. The $E2$ matrix elements in the vicinity of the intersection between the S and γ-vibrational bands are listed in Fig. 10 together with results from a three-band (ground-state, S, and γ-vibrational bands) mixing calculation. The calculations were carried out using the intraband intrinsic matrix element $\langle K|E2|K\rangle = 2.31$ e b for both the ground-state and γ-vibrational bands, 2.77 e b for the S band, and the interband intrinsic matrix element between the ground-state and γ-vibrational bands listed in Table V. The unperturbed level energies were taken from an

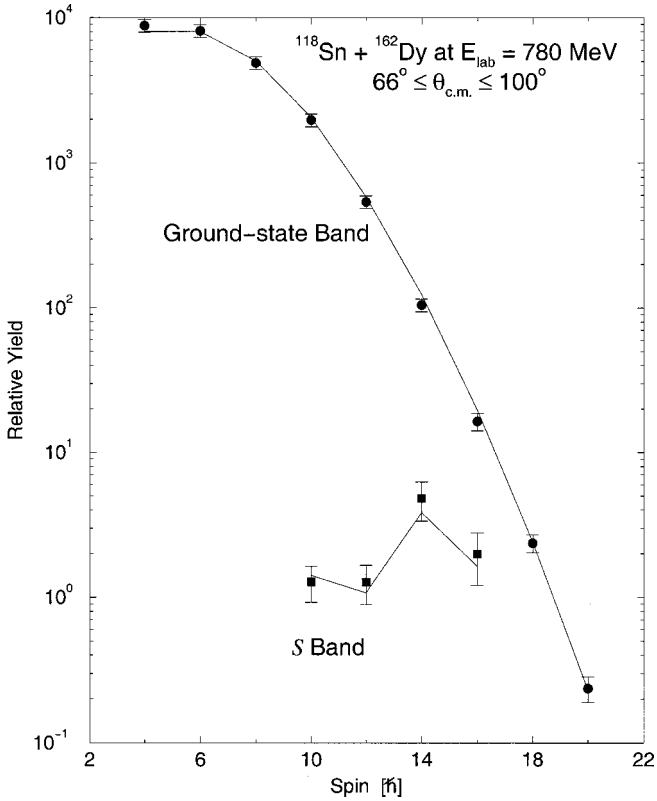

FIG. 7. Comparison of the γ-ray yields between prediction and experiment for the intraband transitions of both the ground-state and S bands. The solid lines are the Coulomb excitation calculations for the best fits to the data.

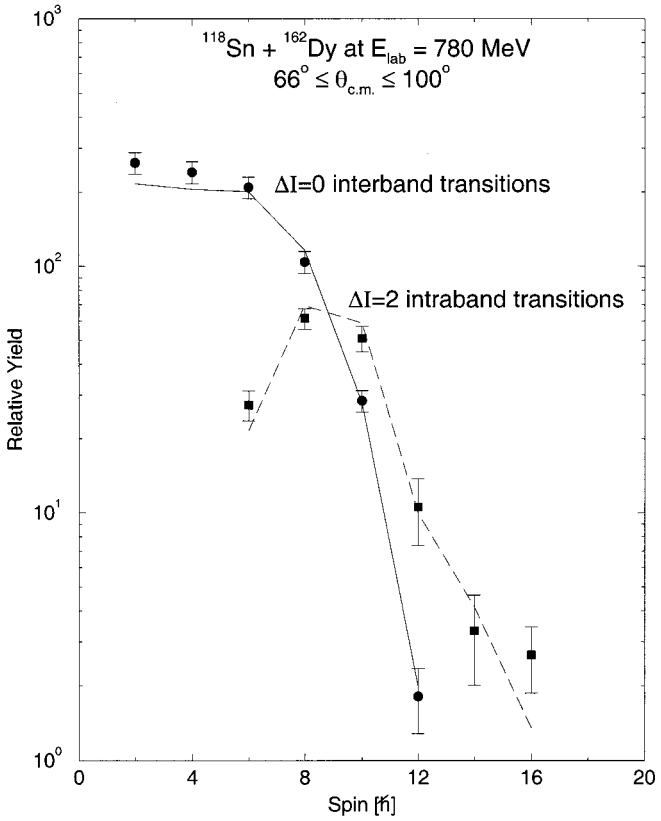

FIG. 8. Comparison of the γ-ray yields between the prediction and experiment for both intraband and interband transitions of the γ-vibrational band. The solid and dashed lines are the Coulomb excitation calculations for the best fits to the data.

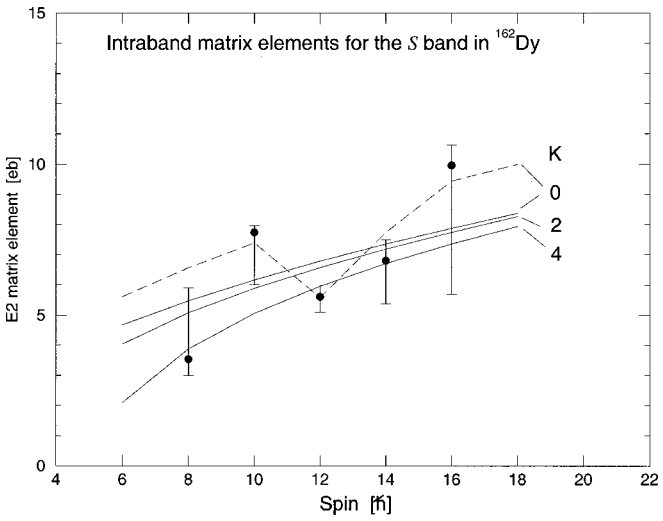

FIG. 9. The $E2$ matrix elements for the $I \rightarrow (I-2)$ transitions of the S band in ^{162}Dy. The solid lines are the rotor values assuming $\langle K|E2|K\rangle = 2.31$ e b. The dashed line is the result of a three-band (ground-state, S, and γ-vibrational bands) mixing calculation assuming a 20% larger intrinsic matrix element for the S band than the one used for the solid line.

interpolation of the smooth curves of moment of inertia shown in Fig. 5. A quantitative agreement is obtained between the measured $E2$ matrix elements and calculations. The determined interaction matrix element between the S and γ-vibrational bands is $\approx$40–45 keV. This compares with 31 keV, determined from the measured branching ratios for the decay of the 12^+_γ listed in Table II according to the description in Ref. [24], which assumes that the quadrupole deformation is the same for both interacting bands.

The electromagnetic properties for states with spin 8^+ to 20^+ in the S band in ^{162}Dy can be summarized as follows.

(1) The quadrupole deformation is $\approx$20% larger than the deformations of the nearby collective bands both from direct comparison of the $E2$ matrix elements with the rotor prediction and from comparison with the three-band-mixing calculation.

(2) Strong mixing with the γ-vibrational band at spin 12^+ is evident from the level repulsion, shown in the plot of moment of inertia vs rotational frequency (Fig. 5), and from the calculated wave function for the 12^+ state of the S band, $|12_s\rangle \approx 0.83|12_s\rangle_{\rm unpert} + 0.53|12_\gamma\rangle_{\rm unpert}$, in the three-band-mixing calculation.

(3) The strong mixing is because of an accidental degeneracy, not a strong interaction, judging by the weakness of the interaction matrix element, $\approx$40–45 keV derived from the three-band-mixing calculation. The S band eventually crosses the ground-state band at 18^+ and the interaction matrix element $\approx$12 keV was derived from the measured γ-ray branching ratios $R[(18^+_s \rightarrow 16^+_1)/(18^+_s \rightarrow 16^+_s)] = 0.30$ according to the description in Ref. [24]. This interaction matrix element is comparable to 17 ± 2 and 18 ± 2 keV obtained by Jungclaus *et al.* [9] and by Bauer [17], respectively.

(4) A low value for the K quantum number of the S band is implied by the dominate $M1$ component and the magnitude of $M1$ matrix elements, $B(M1; 8^+_s \rightarrow 8^+_1)$

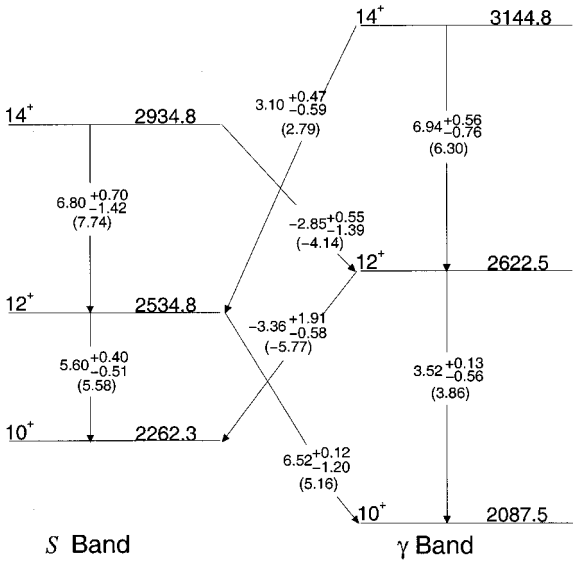

FIG. 10. The determined $E2$ matrix elements for the transitions of the 12^+ and 14^+ states of both the S and γ-vibrational bands. The values in the parentheses result from a band-mixing calculation among the ground-state, S, and γ-vibrational bands.

TABLE VI. Band-head excitation energies of the two $K^\pi=4^+$ bands and their intrinsic matrix elements for the intraband transitions and for the interband transitions to the γ band in ^{162}Dy.

Excitation energy (MeV)	$\langle K=4\|E2\|K=4\rangle$ (e b)	$\langle K=4\|E2\|K=2\rangle$ (e b)	M_2/M_1
1.536	2.28	0.115	-0.0304
2.181	2.19	0.178	(-0.0304)

TABLE VII. Intrinsic matrix elements for the intraband transitions of $K^\pi=2^-$ band and for the interband transitions to both the ground-state and γ bands in ^{162}Dy.

$\langle K^\pi=2^-\|m_{\Delta K=2,\nu=1}\|K^\pi=0^+\rangle$	0.00037 e b$^{1/2}$
$\langle K^\pi=2^-\|E1\|K^\pi=2^+\rangle$	0.0053 e b$^{1/2}$
$\langle K^\pi=2^-\|E2\|K^\pi=2^-\rangle$	2.41 e b
$\langle K^\pi=2^-\|E3\|K^\pi=0^+\rangle$	0.244 e b$^{3/2}$

$=0.0058$ W.u., for example, were measured for the $\Delta I=0$ transitions to the ground-state band.

There are two $K^\pi=4^+$ bands in ^{162}Dy populated in the current experiment. Since both bands decay mainly to the $K^\pi=2^+$ γ-vibrational band, we consider the couplings to the $K^\pi=2^+$ γ-vibrational band to be the only interband transitions pertinent to this study. The interband transitions of the known $K^\pi=4^+$ band at 1535.9 keV to the γ-vibrational band were found to be correlated well by Eq. (1). The M_2/M_1 ratio, listed in Table VI, was determined by the observed branching ratios that are listed in Table III. Thus only one free parameter, that is the absolute intensity, was needed in the analysis for the interband transitions with the ratio M_2/M_1 fixed. The same ratio was assumed for the interband transitions for the new $K^\pi=4^+$ band at 2181.0 keV because the limited data on the decay branching ratios, listed in Table III, are consistent with such systematics. One additional parameter for each band is needed to account for the $E2$ matrix elements within a band, which were assumed to be a rotor and driven by an intrinsic matrix element. The determined intraband and interband intrinsic matrix elements for both $K^\pi=4^+$ bands are listed in Table VI. The uncertainty for the intraband intrinsic matrix element is $\approx$30% and for the interband is $\approx$15%. The analysis of Bauer [17] for a similar experiment gives $B(E2;4^+(1536)\rightarrow 2^+_\gamma)=1.1(2)$ W.u. and $B(E2;4^+(2181)\rightarrow 2^+_\gamma)=4.5(5)$ W.u.. The corresponding $B(E2)$ values from our analysis are 1.15(35) W.u. and 2.78(83) W.u., respectively. Direct comparison between these two studies should be treated with caution as the assumption made on the correlations for the interband transitions is different. The perturbation to the correlations of the interband transitions due to the coupling between the rotation and intrinsic motions is ignored in Bauer's analysis, that is, the ratio $M_2/M_1=0$ is assumed.

The measurable collectivity for the coupling between those $K^\pi=4^+$ bands to the $K^\pi=2^+$ γ-vibrational band can be addressed in the framework of a two-phonon γ-vibrational excitation. Since the mixing of those intrinsic states with two-quasiparticle states may be significant, due to the excitation energies being near or above the pairing gap, one measure of the integrity of two-phonon γ-vibrational state is to compare the intrinsic matrix element of two-phonon to one-phonon excitation using the harmonic two-phonon strength as a yardstick. Comparison in the intrinsic frame is necessary because the non-negligible coupling effect between the rotation and intrinsic motions as discussed in Ref. [25]. The known $K^\pi=4^+$ band at 1535.9 keV accounts for $\approx$11% of the harmonic two-phonon γ-vibrational strength using the determined intrinsic matrix elements listed in Table V and VI and the newly identified $K^\pi=4^+$ band at 2181.0 keV accounts for $\approx$25%. These results are consistent with a highly fragmented two-phonon γ-vibrational excitation in ^{162}Dy.

The only negative-parity band populated in the current experiment is the $K^\pi=2^-$ octupole-vibrational band in ^{162}Dy. This band has the lowest excitation energy and the strongest $E3$ strength, $B(E3;3^-\rightarrow 0^+)=9.5(6)$ W.u. [26], among all the known octupole-vibrational bands, which include $K^\pi=0^-$, 1^-, 2^-, and 3^- bands. Since the $E3$ mode cannot compete with the $E1$ mode for the decay of members of the octupole-vibrational band to those of the positive-parity band, the observed γ-ray decay branchings contain no information on the $E3$ systematics. In contrast, the $E3$ mode is responsible for the population of the negative-parity band by Coulomb excitation. In our analysis, the Alaga rule was assumed for the $E3$ interband matrix elements between the $K^\pi=2^-$ and the ground-state bands. Rotor values were assumed for the $E2$ matrix elements within the band. For the allowed $E1$ transitions to the γ-vibrational band, the Alaga rule was found to be valid in correlating those $E1$ matrix elements derived from the observed ratios of $E1$ transitions to intraband $E2$ transitions. For the forbidden $E1$ transitions to the ground-state band, the $E1$ matrix elements, derived from the observed $E1/E2$ ratios, correlated well using the equation [Eq. (4-95) in Ref. [23]]

$$\langle K'=2,I_{K'}\|E1\|K=0,I_K\rangle=\sqrt{2}(2I_K+1)^{1/2}\times\langle I_K(K'-1)11|I_{K'}K'\rangle,$$

$$\left[\frac{(I_K-K)!(I_K+K+1)!}{(I_K-K-1)!(I_K+K)!}\right]^{1/2}\langle K'|m_{\Delta K=2,\nu=1}|K\rangle. \quad (4)$$

A total of four parameters, one for each group of electromagnetic matrix elements, were used in the fitting to the γ-ray yields.

The intrinsic $E1$, $E2$, and $E3$ matrix elements resulting from this analysis are listed in Table VII. The uncertainty for the $E1$ intrinsic matrix element to the ground-state band is $\approx$15%, for the $E1$ to the γ-vibrational band $\approx$50%, for the $E2$ within a band $\approx$25%, and for the $E3$ to the ground-state band $\approx$20%. The latter implies that the $B(E3)$ for the $3^-\rightarrow 0^+$ transition is 5.5(22) W.u., which is lower than 9.5(6) W.u. measured in Ref. [26] by 1.75 standard deviation. However, one has to bear in mind that the current analysis emphasizes the average $E3$ strength over the individual strength for the transitions between the $K^\pi=2^-$ octupole-vibrational

and the ground-state band. This result may suggest the existence of a non-negligible spin-dependent term in the $E3$ systematics. The $E1$ intrinsic matrix element obtained for the forbidden transitions to the ground-state has a similar magnitude to those found in the neighboring nuclei of ^{162}Dy [26].

V. SUMMARY

The electromagnetic properties for ^{162,164}Dy have been studied using projectile excitation by a ^{118}Sn. The significantly enhanced detection efficiency for both scattered heavy ions and γ rays in this experiment, provided by the combination of GAMMASPHERE and CHICO, has allowed study of nuclear structure to higher excitation energy and spin and in greater detail than previously attained. One of the most distinct results is the first measurement of electromagnetic properties of the S band for states with spin 8^+ to 20^+, that is, well below the crossing with the ground-state band. The strong mixing between the S and the γ-vibrational bands in ^{162}Dy allowed such study by Coulomb excitation. The quadrupole deformation of the S band between spin 8^+ and 20^+ was found to be $\approx$20% more deformed than observed for the nearby low-lying collective bands. In addition, other aspects of collectivity, such as the two-phonon γ-vibrational excitation and the octupole-vibrational excitation also were addressed by the current experiments. A highly fragmented two-phonon γ-vibrational excitation was found in ^{162}Dy with 36% of the harmonic two-phonon strength distributed among the lowest two $K^\pi=4^+$ bands. Significant $E3$ strength was observed coupling the ground-state band to the $K^\pi=2^-$ octupole-vibrational band.

ACKNOWLEDGMENTS

We thank Dr. K. Gregorich and Dr. M. A. Stoyer for making and handling the ^{252}Cf source for the CHICO calibration. The work by the Rochester group was funded by the National Science Foundation. The work at LBNL was performed under the auspices of the Department of Energy under Contract No. DE-AC03-76SF00093.

[1] F.S. Stephens and R.S. Simon, Nucl. Phys. **A183**, 257 (1972).
[2] R. Bengtsson, I. Hamamoto, and B. Mottelson, Phys. Lett. **73B**, 259 (1978).
[3] J. Almberger, I. Hamamoto, and G. Leander, Phys. Lett. **80B**, 153 (1979).
[4] H. Emling, E. Grosse, D. Schwalm, R.S. Simon, H.J. Wollersheim, D. Husar, and D. Pelte, Phys. Lett. **98B**, 169 (1981).
[5] H. Emling, E. Grosse, R. Kulessa, D. Schwalm, and H.J. Wollersheim, Nucl. Phys. **A419**, 187 (1984).
[6] A. Pakkanen *et al.*, Phys. Rev. Lett. **48**, 1530 (1982).
[7] J. Gen-Ming, J.D. Garrett, G. Lovhoiden, T.F. Thorsteinsen, J.C. Waddington, and J. Rekstad, Phys. Rev. Lett. **46**, 222 (1981).
[8] S.W. Yates *et al.*, Phys. Rev. C **21**, 2366 (1982).
[9] A. Jungclaus *et al.*, Prog. Part. Nucl. Phys. **46**, 213 (2001).
[10] C.Y. Wu, M.W. Simon, D. Cline, G.A. Davis, A.O. Macchiavelli, and K. Vetter, Phys. Rev. C **57**, 3466 (1998).
[11] M.W. Simon, D. Cline, C.Y. Wu, R.W. Gray, R. Teng, and C. Long, Nucl. Instrum. Methods Phys. Res. A **452**, 205 (2000).
[12] M.W. Simon *et al.*, in *Proceedings of the International Conference on Fission and Properties of Neutron Rich Nuclei, Sanibel Island, Florida*, edited by J.H. Hamilton and A.V. Ramayya (World Scientific, Singapore, 1998), p. 270.
[13] K. Vetter *et al.*, Phys. Rev. C **58**, R2631 (1998).
[14] C.Y. Wu, D. Cline, M.W. Simon, R. Teng, K. Vetter, M.P. Carpenter, R.V.F. Janssens, and I. Wiedenhover, Phys. Rev. C **61**, 021305(R) (2000).
[15] R.G. Helmer and C.W. Reich, Nucl. Data Sheets **87**, 317 (1999).
[16] M.W. Guidry, I.Y. Lee, N.R. Johnson, P.A. Butler, D. Cline, P. Colombani, R.M. Diamond, and F.S. Stephens, Phys. Rev. C **20**, 1814 (1979).
[17] H. Bauer, Ph.D. thesis, Heidelberg University, 1998.
[18] C.A. Fields, K.H. Hicks, R.A. Ristinen, F.W.N. de Boer, P.M. Walker, J. Borggreen, and L.K. Peker, Nucl. Phys. **A389**, 218 (1982).
[19] E.N. Shurshikov and N.V. Timofeeva, Nucl. Data Sheets **65**, 365 (1992).
[20] F. Kearns, G. Varley, G.D. Dracoulis, T. Inamura, J.C. Lisle, and J.C. Willmott, Nucl. Phys. **A278**, 109 (1977).
[21] T. Czosnyka, D. Cline, and C.Y. Wu, GOSIA users manual UR-NSRL-305, 1991.
[22] D. Cline, Annu. Rev. Nucl. Part. Sci. **36**, 683 (1986).
[23] A. Bohr and B.R. Mottelson, *Nuclear Structure* (Benjamin, Reading, MA, 1975), Vol. II.
[24] G.B. Hagemann and I. Hamamoto, Phys. Rev. C **46**, 838 (1992).
[25] C.Y. Wu and D. Cline, Phys. Lett. B **382**, 214 (1996).
[26] F.W. McGowan and W.T. Milner, Phys. Rev. C **23**, 1926 (1981).
[27] M.J.A. de Voigt, J. Dudek, and Z. Szymanski, Rev. Mod. Phys. **55**, 949 (1983).